

Who Brings the Frisbee: Probing Hidden Hallucination Factors in Large Vision-Language Model via Causality Analysis

Po-Hsuan Huang^{1*}, Jeng-Lin Li^{1*}, Chin-Po Chen¹, Ming-Ching Chang^{1,2}, Wei-Chao Chen¹

¹Inventec Corporation, ²University at Albany - SUNY

¹No. 66, Hougang St., Shihlin Dist., Taipei City, ²Albany, New York

¹{huang.reese, li.johncl, chen.jackcp, chang.ming-ching, chen.wei-chao}@inventec.com,

²mchang2@albany.edu *

Abstract

Recent advancements in large vision-language models (LVLM) have significantly enhanced their ability to comprehend visual inputs alongside natural language. However, a major challenge in their real-world application is hallucination, where LVLMs generate non-existent visual elements, eroding user trust. The underlying mechanism driving this multimodal hallucination is poorly understood. Minimal research has illuminated whether contexts such as sky, tree, or grass field involve the LVLM in hallucinating a frisbee. We hypothesize that hidden factors, such as objects, contexts, and semantic foreground-background structures, induce hallucination. This study proposes a novel causal approach: a hallucination probing system to identify these hidden factors. By analyzing the causality between images, text prompts, and network saliency, we systematically explore interventions to block these factors. Our experimental findings show that a straightforward technique based on our analysis can significantly reduce hallucinations. Additionally, our analyses indicate the potential to edit network internals to minimize hallucinated outputs.

1. Introduction

Large vision-language models (LVLM) can comprehend multimodal data and respond to human commands [8,21,45,54]. Alongside advancements in network architectures, significant research focuses on improving response accuracy and reducing deviations from human instructions [8, 21]. Despite these efforts, modern LVLMs struggle with real-world challenges due to their notorious hallucinations [2, 22] jeopardizing downstream reliability and safety.

LVLM hallucinations occur when the generated contents do not align with the provided visual cues or include unrelated or incorrect texts [22]. Mitigating hallucinations

by fine-tuning LVLMs with human preferences is effective but expensive, requiring extensive human annotations [49]. To reduce costs, recent research employs auxiliary models, such as object grounding and language refinement models, to automatically generate pseudo annotations [47]. Alternatively, approaches that require LVLMs to answer multiple verification questions iteratively incur significant computational overhead [38]. Besides directly optimizing human preferences, post-training inference calibration, for example, enforcing the decoding with contrast to erroneous variations, can partly reduce hallucination probability [14].

Despite various strategies proposed to reduce hallucination in LVLMs, a limited understanding of their response behaviors still hinders further research. Clearly, various uncontrolled hidden factors contribute to these intricate hallucinations when the LVLMs process multi-modality data. For example, Figure 1 shows an example where InstructBLIP [8] erroneously describes a nonexistent frisbee. This mistake likely arises from the presence of a large green grass field in the photo, where frisbees frequently co-occur in the training data. Spurious correlations lead to cross-modality retrieval errors, where models predict objects based on their frequent occurrences in training data [12]. Mitigating these errors requires fine-grained data augmentation and balancing across modalities [4]. Additionally, poor image-text alignment biases the decoding mechanism towards language, which tends to neglect image contents [11, 14]. Analytical studies, such as [53], have identified factors like occurrence, uncertainty, and object position through statistical analyses, but lack a unified framework to analyze the hidden factors inducing hallucination. These studies have not scrutinized hidden context factors, such as the people, trees, or grass in the image, that might induce hallucinations.

It is crucial to understand the conditions that lead to LVLM hallucinations and analyze their **causal patterns**. When there are green fields, it is likely to have a frisbee in the training data, leading to the hallucination mentioned

*The first two authors equally contribute to this work.

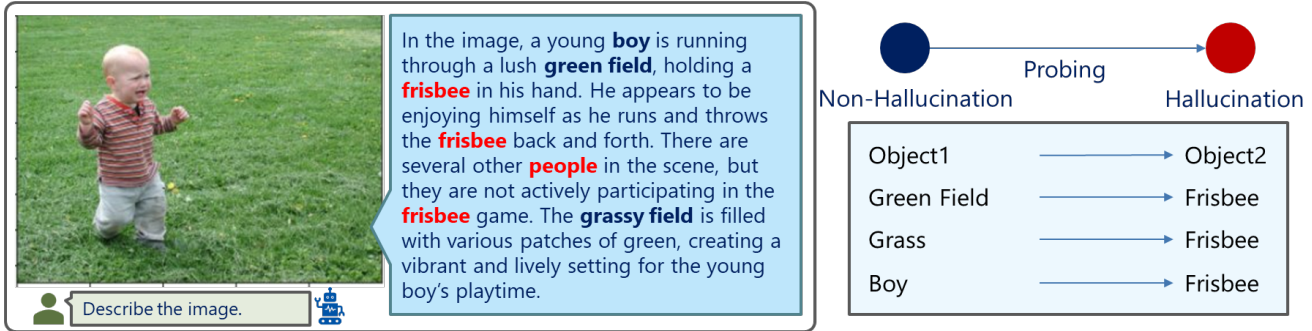


Figure 1. The InstructBLIP [8] LVM hallucinates a frisbee when describing a boy in the green field. There might be a spurious correlation between a boy and a frisbee. Meanwhile, the green field is another non-hallucinatory subject that might induce hallucinations. This underlying relation remains underexplored in the hallucination reduction research.

above in Figure 1. However, the reverse scenario is less likely, due to the relatively fewer training data focusing mainly on frisbees. Additionally, there is a significant gap in studies connecting hallucination analysis with hallucination reduction strategies. To address this, we systematically investigate four fundamental research questions about LVM hallucination concerning visual objects: (1) Are semantic structures affecting hallucination? (2) What are the effects of non-hallucinated objects that are potentially accompanied by hallucinated objects? (3) How likely can we intervene in LVM regarding hallucinated objects to reduce the effects of hidden factors? (4) Are there salient network internals implying network hallucination?

This study explores object hallucination patterns and introduces a novel causal intervention scheme to analyze LVM behaviors. We examine the causal relations between visual objects in the dataset and observe the generated LVM outputs, overviewed in Figure 3. Our findings highlight the key relations between a main subject and the context. We demonstrate that simple intervention to the observed structures can notably reduce hallucinations. Additionally, we investigate the network internal saliency of latent embeddings based on causally-related inputs. Our analysis results pave the way for seamless interference in model generation to mitigate hallucination occurrences.

Our contributions are summarized in the following:

- Investigating hallucination relations between hallucination-inducing words and hallucinatory words
- Identifying a unified causality graph to develop hallucination reduction solutions
- Analyzing intervention on text, image, and embedding
- Probing embedding properties of high-hallucinatory and non-hallucinatory images

2. Related Work

2.1. Large Vision-Language Model (LVM)

Large pre-trained models have heralded a new era of vision language models. InstructBLIP [8], mPLUG-Owl [44,

45], MiniGPT [54], and LLaVa [21] all leverage autoregressive pre-trained large language models (LLMs) paired with fine-tuned vision encoders and multimodal alignment modules. Researchers construct extensive instruction datasets for instruction tuning, aiming to enhance response quality [21]. Additionally, automatic instruction generation approaches can effectively scale up training [36]. Despite addressing known shortcomings of models, challenges persist in fully understanding their behaviors.

2.2. Hallucination Detection and Elimination

Mitigating hallucination issues was initially studied in the field of image captioning and later extended to LVMs. Traditional image captioning metrics such as CIDEr [34] and METOER [3] often fail to capture the object hallucination within a sentence. The polling-based hallucination detection method (POPE) involves a large set of questions asking whether a specific object is present in an image [16]. Despite the LVM evaluation rapidly expanding to various types of hallucinations [30, 33, 40], the fundamental issue of visual object hallucination remains unsolved.

Instruction tuning: LRV-Instruction [20] dataset is designed to balance positive and negative instructions for robust instruction tuning. Direct preference optimization improves the model using annotated data of both hallucinated and non-hallucinated samples, supported by a reward model providing feedback during fine-tuning [9]. However, the quality of collected instructions and the computational overhead continue to be major inconveniences.

Self-check and auxiliary models: Volcano [13] is a self-feedback guided revision model that iteratively asks itself questions to improve response quality. To mitigate the self-bias of LVMs leading to hallucinations, object existence verification can be achieved by prompting another open-vocabulary object detector [41, 51]. These verification results serve as a reward model during LVM fine-tuning. More complex multiple-step strategies including question generation, object grounding, and language refinement are subsequently designed [46, 47]. These methods avoid up-

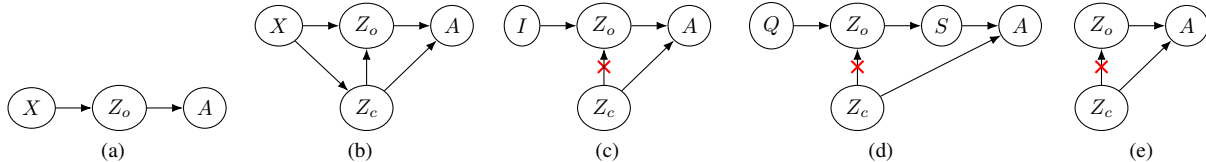


Figure 2. (a) Ideal LVM generation. (b) The **causal graphical model for LVM generation**. (c-e) Deconfounded by (c) image intervention, (d) text intervention, and (e) embedding intervention.

dating model parameters, relying on regenerated or refined answers from ChatGPT [1], indicating their success hinges on the strong summarization ability of ChatGPT. We observe that discriminative ability in vision question answering does not directly indicate generative hallucination (reported in supplementary). Hence, we focus on hallucination in the generative task for our framework design.

Post-training adjustment methods: Recent studies investigate various decoding strategies, including *contrastive decoding* [14] and beam search strategies [10]. VCD [14] calibrates output predictions by contrasting the output distribution between original and distorted visual inputs. OPERA [10] explores related patterns in attention outputs and removes candidate words exhibiting aggregation patterns to prevent decoding hallucination words. Some previous works investigate post-training *calibration* methods to avoid the cost of fine-tuning. For instance, Lin et al. [18] calibrates predictions by estimating linguistic bias in the training data. While recent LLM studies address hallucinations through probing and editing strategies [6, 15], these approaches have not been explored in LVLMs.

Causality provides a robust framework for uncovering hidden inference structures. The Structural Causal Model (SCM) [27] has been widely employed in debiasing LLMs to unveil inherent causal relations between data and labels [52]. A causal attention mechanism was developed to mitigate unobserved confounding factors in vision-language Transformers [43]. Additionally, causal effects are also integrated into loss functions to address counterfactual biases [35]. However, the hallucination phenomenon in LVLM remains under-investigated due to the naturally complex multimodal structure, hindering systematic understanding. Most previous studies focus on vision-language discriminative tasks with clear binary targets [5, 24, 25] or short generated sequences in image captioning tasks [19, 42]. There is a lack of exploration into causal structures for hallucination patterns in generative tasks.

3. Method

3.1. Datasets, LVM Setup, and Hallucination Evaluation Metrics

Datasets: We utilize the AMBER dataset [37] and COCO dataset [17] for evaluation. AMBER is a benchmark dataset assessing LVM hallucination, including human annotations on both truly appeared objects and potentially hal-

lucinated ones. The setting of COCO is followed by prior works [10] with randomly selected 500 images from the 2014 validation set. Here, we prompt LVLMs with “Describe this image.” to obtain descriptions for the images.

Large vision-language model (LVLM): We utilize an auto-regressive transformer-based LVLM denoted as f . The input token sequence $X \in \mathbb{R}^{N \times T}$ with N samples and T timesteps is fed into the LVLM to the latent embedding $E \in \mathbb{R}^{N \times T \times D}$ for D latent dimensions and generate the text $A = f(X)$. We employed two established LVLMs including InstructBLIP [8] and mPLUG-Owl2 [45].

Hallucination evaluation metrics: The evaluation function H assigns a hallucinatory score $H(A) \in \mathbb{R}$ to a response A , indicating hallucination rates with given metrics. We follow the metrics used in the dataset papers for evaluation. We assess LVLM hallucination using several common metrics: CHAIR, Cover, HAL, and Cog scores on AMBER dataset [37] as well as CH_i , CH_s , and Recall on COCO [10]. CHAIR [31] measures the hallucination generation rate. CH_i and CH_s , represent the image-level and sentence-level hallucination rates, respectively. Cover and Recall measure the ratio of mentioned existing objects to all existing objects in the image. HAL indicates whether the CHAIR score is non-zero for a sentence. Cog measures the hallucinatory object rate resembling human cognition.

3.2. Hallucination Statistics

We investigate the hallucination results using human-annotated labels from the AMBER dataset to illustrate the underlying data and model properties. Table 1 lists the top 5 most common hallucination cases, including a *single-hallucinatory* word, *co-occurring hallucinatory* words, and the *hallucinatory-inducing* words. The hallucinatory-inducing words are non-hallucinatory while associated with other hallucinatory words. These cases were detected using InstructBLIP and mPLUG-Owl2 on the AMBER dataset, suggesting that LVLMs exhibit different hallucination inclinations.

Co-occurring hallucinatory words: Frequently hallucinated words tend to co-occur with other hallucinated words. Once a hallucination occurs, other hallucinations are likely to follow. We present the top 5 most common co-occurring hallucination words in Table 1 (b). Observe that co-occurring hallucinatory words differ from single-hallucinatory words. The appearance of these paired hal-

| InstructBLIP | | | | | | mPLUG-Owl2 | | | | | |
|--------------|----|---------------------|----|-----------|----|------------|----|--------------------|----|-----------|----|
| (a) O_h | # | (b) O_h^1, O_h^2 | # | (c) O_n | # | (a) O_h | # | (b) O_h^1, O_h^2 | # | (c) O_n | # |
| people | 68 | (people, O_h^2) | 68 | tree | 60 | people | 88 | (people, O_h^2) | 40 | water | 41 |
| person | 34 | (person, O_h^2) | 41 | water | 52 | bottle | 40 | (cup, O_h^2) | 40 | tree | 39 |
| car | 25 | (cup, O_h^2) | 26 | sky | 32 | car | 38 | (bottle, O_h^2) | 39 | road | 38 |
| tree | 21 | (bottle, O_h^2) | 25 | beach | 31 | person | 31 | (person, O_h^2) | 39 | beach | 32 |
| sun | 21 | (bicycle, O_h^2) | 22 | road | 31 | chair | 24 | (book, O_h^2) | 30 | people | 27 |

Table 1. This table shows the counts of the top 5 frequent (a) *single-hallucinatory* words O_h , (b) *co-occurring hallucinatory* words (O_h^1, O_h^2) (c) *Hallucinatory-inducing* words O_n . O_n is frequently associated with other hallucinatory words O_h , i.e., $O_n \rightarrow O_h$. # denotes the counts of the word. See Supplementary for full results.

lucinated words is usually syntactically correct in image descriptions, which might be one reason that paired co-occurrence words appear. These observations suggest that the underlying syntactic and semantic structures influence the relationships between words of hallucinations.

Hallucinatory inducing words: Aside from the co-occurrence of hallucinatory words, we are also interested in an important causal factor “What induces a hallucination?”. Given a generated response A , the mentioned object set is denoted as $S = \{s_1, \dots, s_n\}$ and the ground-truth object set is $O = \{o_1, \dots, o_m\}$. The hallucinatory words are the objects absent in the ground-truth object set, i.e., $O_h = S \setminus O$, and the set of non-hallucinatory words is denoted as $O_n = S \cap O$. We regard the unrevealed relation between hallucinatory and non-hallucinatory words using conditional probability $P(O_h | O_n)$ [28]. Table 1 (c) shows the $O_n \rightarrow O_h$ relations in AMBER. Words like ‘tree’, ‘water’, ‘sky’, ‘beach’, and ‘road’ are scene-like nouns, which usually describe the background information. The appearance of these types of nouns often induces other hallucinatory words. For example, a tree induces a bicycle to hallucinate probably because they are likely to appear in the same scene. However, the observed hallucination word relations remain unclear regarding causality, raising concerns about spurious correlations and risks of misinterpretation. Therefore, we utilize the causality analysis to identify solutions for hallucination reduction.

3.3. Causality Analysis

We formulate a causal graphical model involving the input random variables: image I , text query Q , a latent variable of target object Z_o , context factor Z_c , and the resulting answer A . This model is represented by a directed acyclic graph (DAG) as shown in Figure 2. In this graph, a directed edge between variables indicates a direct causal influence of the parent node on the child node.

We distinguish and abstract the variables Z_o and Z_c at a cognitive level. Z_o represents the ideal semantic representation of target objects (e.g., the concept of a car), while Z_c as a **confounding** variable denotes a context pattern that could diversify the comprehension of the car. Figure 2a depicts

an ideal LVLM generation, where A is independent of Z_c . However, the inherent bias in the training data introduces Z_c into the **causal graphical model for LVLM generation** in Figure 2b, shaping the unwanted causal effect $Z_c \rightarrow Z_o$.

We adopt the standard causality analysis approach [27, 29]; performing an intervention on input nodes to block the undesired effects from the confounding factor Z_c . We set up the causal effect metric $\delta(P, P')$ between a distribution P and the distribution after intervention P' is defined as the fewer hallucinations after the intervention; that is, $\delta = \mathbb{I}(H(A) > H(A'))$, where A' denotes the resulting answer after the intervention and H is the hallucination evaluation metric defined in §3.1. The causal effect metric δ reflects whether an intervention successfully reduces hallucination. We measure the **total causal effect (TCE)** [26, 32] over an evaluation test set. For the intervention results, TCE calculates the expected value \mathbb{E} of δ over the evaluation test set X by the equation:

$$TCE = \mathbb{E}_{x' \sim \mathbb{P}(X)}[\delta(P, P')], \quad (1)$$

Based on the causal relation depicted in Figure 2, we can leverage intervention approaches to interrupt the undesired effects of Z_c . The intervention is denoted as $do(X : x \rightarrow x')$ and simplified as $do(X)$, where x and x' are inputs before and after an intervention. The path $Z_o \leftarrow Z_c \rightarrow A$ forms a backdoor path and thus we aim to perform an intervention to block the path $Z_c \rightarrow Z_o$. To achieve this, we consider intervening image I (§3.4), text query Q (§3.5), or latent embedding E (§3.6), shown in Figure 3 and described in the following subsections.

3.4. Image (I) Intervention

In Figure 2c, the effect of the query text Q is minimized by using a fixed, simple prompt as described in §3.3. This allows us to focus on the interactions between I , Z_o , Z_c , and A . We aim to perform intervention $do(I)$ on the image I while assuming that the image after intervention I' minimally changes Z_c . Formally, we assume that $P(Z_c | I') \approx P(Z_c | I)$. This assumption holds if I' primarily affects Z_o and has a much weaker effect on Z_c . We

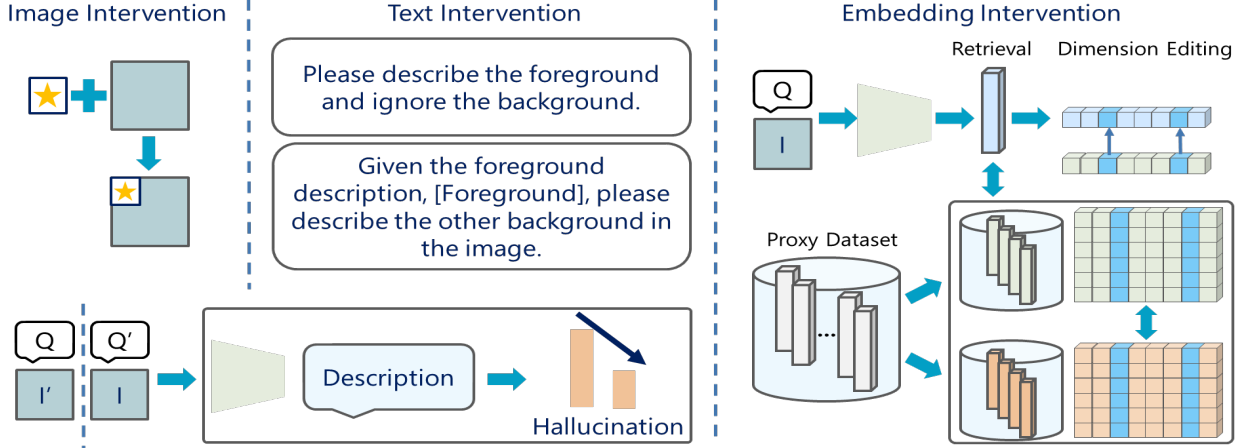


Figure 3. Our proposed image, text, and embedding intervention approaches correspond to Figure 2 (c), (d), and (e).

expect this to hold in our design, which involves small object modifications and focuses on the region related to Z_o .

The confounding effect of Z_c can thus be mitigated using the backdoor adjustment. We can examine the TCE based on Eq. (1) with $P' = \mathbb{P}(A|Q, do(I))$. We implement this image intervention $do(I)$ using two different object manipulation designs: pasting a small object in the background of I , based on the observation of the differing hallucinatory tendencies of LVLMs regarding the target objects and the rest context elements, as shown in Figure 3; and removing a hallucinatory-inducing object from I where the object is specified by statistics in §3.2. Specifically, for the *image-pasting* intervention, we paste a small image featuring a single object, sized to one-sixth of the shortest side of I , at the top left corner. This ensures the object is recognizable and in the background, implicitly affecting Z_o . For the *object removal* intervention, we remove one hallucinatory-inducing object in the image based on the highest hallucinatory frequency $\sum_{o_i \in O_h} P(o_i | O_n)$, where O_n is the non-hallucinatory object set and O_h is its corresponding hallucinatory object set. We report these prior statistics in Table 1. For example, if ‘person’ is a non-hallucinatory object, it is most likely associated with a hallucinatory object; thus, it has the highest priority for removal when present in I . We utilize the combination of the GroundingDINO [23] and IA [48] to detect and segment the object and then fill the masked area using the inpainting technique.

3.5. Text (Q) Intervention

Our proposed text intervention technique comprises two steps, separately prompting for the foreground (FG) and background (BG) generation. This **foreground-background (FGBG)** technique is designed based on the idea of interrupting the effects from Z_c via changing the object concepts Z_o on the backdoor path, $Z_o \leftarrow Z_c \rightarrow A$ shown in Figure 2d. We directly intervene in the text

query as Q' with the FGBG strategy and thus Z'_o changes accordingly, paving an alternative causal way to prevent Z_c from affecting Z_o . The quantified TCE of Q intervention involves the $P(A|do(X))$ probability distribution. Our designed **FGBG** approach is a Chain-of-Thought (CoT)-like prompting technique with the front-door adjustment [29, 50]. By introducing a mediator variable S to perform the two-step prompting, the probability distribution to generate A becomes as below:

$$P(A|do(X)) = \sum_S P(A|do(S))P(S|do(X)). \quad (2)$$

This approach avoids the intractable access to variable Z_c as the context variable Z_c can hardly be specified. Therefore, we seek an estimation of the term $P(S|do(X))$ and $P(A|do(S))$ for tractable results. Here, $P(S|do(X))$ and $P(A|do(S))$ correspond to the **FG** and **BG**, respectively.

First, $P(S|do(X))$ is computed in the path of $X \leftarrow Z_c \rightarrow A \leftarrow S$ between X and S . The collision structure of $Z_c \rightarrow A \leftarrow S$ allows us to block the backdoor path and derive $P(S|do(X)) = P(S|X)$. Second, $P(A|do(S))$ is computed by blocking the path $S \leftarrow X \leftarrow Z_c \rightarrow A$ using backdoor adjustment: $P(A|do(S)) = \sum_X P(X)P(A|S, X) = \mathbb{E}_X[P(A|S, X)]$. Instead of navigating the unconstrained space of X , we follow the estimation based on the expectation value of X [39].

$$\mathbb{E}_X[P(A|S, X)] \approx P(A|S, \mathbb{E}[X]) \approx P(A|S \oplus \mathbb{E}[X]), \quad (3)$$

where \oplus denotes vector concatenation. We avoid multiple iterations to form a CoT by specifying the prompt to represent Z_o and minimize the variation. Our observed foreground-background description structure and the non-hallucinatory tendency of the first sentence [53] ensure FG to be specific and consistent. We thus empirically use X in a single run to replace $\mathbb{E}[X]$.

Finally, Eq. (2) can be rewritten as: $P(A|do(X)) = \sum_S P(S|X)P(A|s \oplus \mathbb{E}[x])$. The final intervention result is decomposed into FG $P(S|X)$ and a contextual background (BG) prompt depending on FG, $P(A|s \oplus \mathbb{E}[X])$. Detailed prompts are written in the supplementary.

3.6. Embedding Intervention

Our embedding intervention approach inspired by model editing research [7, 15] can generate a direct intervention to Z_o in Figure 2e without model parameter updates. Depending on samples X in a proxy dataset with hallucination annotations, we derive a hallucinated group $X_h = \{x \in X | H(f(x)) > 0\}$ and a non-hallucinated group $X_n = \{x \in X | H(f(x)) = 0\}$. The corresponding embeddings for X_h and X_n are denoted as E_h and E_n . In contrast to other studies aiming to edit specific words, our targeted generative tasks lack fixed ground truth. Therefore, we propose to measure salient latent embedding dimensions in terms of hallucination and edit these dimensions by retrieving values of the dimensions from non-hallucinated data.

Embedding saliency map: We measure the saliency dimensions over the whole sequence via statistical significance. Specifically, we utilize the Student’s t-test to examine each dimension between E_h and E_n . We select the dimensions with a p-value smaller than 0.001 and derive the saliency maps $M \in \mathbb{R}^{T \times D}$ indicating the dimensions statistically significant in discriminating hallucination and non-hallucination groups in the proxy dataset.

Embedding editing: We calculate the distance between a query embedding E_q and the proxy non-hallucinated embeddings E_n from X_n . The average embedding E_k of the most similar top- K embedding is then selected through the l_2 -distance k-nearest neighbor approach. $\mathbb{E}_K = \frac{1}{K} \sum_{i=1}^K E_i$. Each query sample obtains the mean embedding from most similar and non-hallucinated samples in the proxy dataset. Then, E_K serves as a non-hallucinated prototype to edit the identified hallucination embedding saliency map M . Therefore, the derived embeddings become: $E'_q = (1 - \rho) * E_q + \rho * M * E_K$, where ρ denotes a hyperparameter determining editing strength. The embedding E'_q is then used to decode the output texts A' . This embedding editing technique is an intervention to Z_o to lessen the effects of Z_c in Figure 2b.

4. Experiments

We carry out experiments to show the impact of interventions on reducing hallucinations as detailed in §3.4, §3.5, and §3.6. Our comparisons are aligned with previous studies on hallucination reduction using the AMBER dataset [37] and COCO validation subset. We test our three intervention approaches on InstructBLIP [8] and mPLUG-Owl2 [45] using the default parameter settings of the original paper. For mPLUG-Owl2, we set the hyperparameters

temperature and max new tokens to 0.7 and 512, respectively, to derive similar results in AMBER benchmark [37].

Baselines: We compare our approach with the following baselines: (1) Opera [10]: reduces hallucinations by lowering the attention weight on the summary tokens based on observation occurring on these tokens. (2) VCD [14]: distorts detected hallucinated objects and performs contrastive decoding to avoid generating these objects.

4.1. Evaluation of Image Intervention

We evaluate our *image-pasting and object-removal* intervention methods (§3.4) for reducing LVLM hallucinations. The image-pasting intervention uses a single rabbit as the pasted object. Table 2 compares our method with two state-of-the-art approaches (Opera and VCD) using two LVLMs (InstructBLIP and mPLUG-Owl2). Our method shows consistent improvements in reducing hallucinations on both LVLMs across the AMBER and COCO datasets and performs comparably to Opera and VCD. This supports our finding that focusing LVLMs away from non-informative backgrounds reduces hallucinations.

We also explore various pasting factors, such as style and semantic relationships, using the COCO dataset; see Table 3. We find that inpainting, which blends the pasted object into the background, achieves a more consistent style than direct pasting. For semantic pasting and inpainting, we use objects from the same or different supercategories as the original image. Specifically, non-semantic pasting, such as inserting a bird into a kitchen image, performs better by reducing spurious correlations, while semantic inpainting, which inserts objects with similar semantics, tends to increase related hallucinations.

In contrast, the object removal intervention, as shown in Table 2, results in lower CHAIR and HAL scores but achieves a high Cover rate and a comparable Cog score on the AMBER dataset. Object removal may not effectively reduce hallucinations due to complications like residual background after removing large objects, which can lead to additional hallucinatory artifacts. To better understand the impact of object removal, we also measure its effect on frequently hallucinated objects and their associated inducing words. These findings are detailed in the Supplementary materials.

4.2. Evaluation of Text Intervention

We compare the overall hallucination rate and coverage rate in Table 2. Our proposed *Foreground-Background (FGBG) prompt* can be separated into *FG* and *BG* steps as described in §3.5. We additionally consider another baseline: *Stop prompt* provides a hint for non-existing objects for the model by the prompt: “There are no $[O_h]$ in the image. Then, describe the image.” The object terms O_h are derived from a prior output of LVLM on the same sample

| LVL M | InstructBLIP | | | | | | | mPLUG-Owl2 | | | | | | | |
|-----------------|-----------------|-------------|-------------|------------|-------------|------------|-------------|------------|-------------|-------------|------------|-------------|------------|-------------|---------|
| | Dataset Metrics | Amber | | | | COCO | | | Amber | | | | COCO | | |
| | | CHAIR↓ | Cover↑ | HAL↓ | Cog↓ | CHAIRs↓ | CHAIRi↓ | Recall↑ | CHAIR↓ | Cover↑ | HAL↓ | Cog↓ | CHAIRs↓ | CHAIRi↓ | Recall↑ |
| Baseline | 9.0 | 52.4 | 38.8 | 4.5 | 58.6 | 16.1 | 73.1 | 9 | 53 | 40.4 | 5 | 60.2 | 17.5 | 76.1 | |
| Opera | 8.5 | 52.6 | 37.5 | 4.0 | 41.0 | 11.2 | 71.7 | 9 | 49.8 | 36.1 | 3.7 | 48.8 | 15.0 | 71.6 | |
| VCD (sampling) | 20.3 | 52.1 | 58.5 | 7.1 | 54.6 | 25.8 | 61.7 | 9.9 | 52.6 | 42.4 | 5.3 | 63.0 | 18.3 | 76.6 | |
| Image pasting | 5.5 | 47.8 | 27.2 | 2.7 | 40.4 | 12.3 | 68.5 | 6.4 | 44.7 | 29.0 | 2.5 | 49.6 | 16.3 | 71.7 | |
| object removal | 11.7 | 56.8 | 46.2 | 4.1 | 48.8 | 15.0 | 75.9 | 12.9 | 54.0 | 46.0 | 4.5 | 59.9 | 19.6 | 78.6 | |
| Stopping prompt | 5.1 | 46.7 | 20.0 | 1.9 | 21.6 | 8.2 | 61.7 | 5.5 | 49.7 | 25.0 | 2.4 | 41.0 | 12.4 | 72.8 | |
| FGBG prompt | 5.6 | 53.2 | 27.8 | 2.6 | 27.4 | 7.0 | 68.7 | 5.6 | 54.3 | 26.5 | 2.1 | 30.2 | 9.5 | 69.7 | |
| BG prmopt | 6.4 | 52.4 | 27.1 | 2.6 | 11.2 | 8.4 | 41.0 | 7.8 | 39.7 | 19.6 | 1.7 | 20.4 | 14.2 | 43.9 | |
| Embedding | 8.1 | 52.7 | 33.6 | 3.8 | 50.7 | 14.9 | 72.4 | 8.6 | 51.9 | 33.4 | 4.2 | 55.6 | 15.7 | 75.4 | |

Table 2. Hallucination evaluation on AMBER and COCO datasets using InstructBLIP and mPLUG-Owl2. Compared baselines are presented in the upper part and our proposed text and image intervention results are in the lower part.

| COCO | CHAIRs↓ | CHAIRi↓ | Recall↑ |
|-------------------------|-------------|-------------|-------------|
| mPLUG-Owl2 | 60.2 | 17.5 | 76.1 |
| semantic pasting | 55.4 | 15.8 | 85.2 |
| Non-semantic pasting | 44.8 | 12.1 | 96.6 |
| semantic inpainting | 63.2 | 19.0 | 78.1 |
| Non-semantic inpainting | 51.8 | 14.5 | 89.5 |

Table 3. Results of image pasting intervention with mPLUG-Owl2 on COCO dataset.

which is compared with the annotated ground-truth. This is a hard upper bound for intervention and suggests the possibility of hardly corrected samples.

In Table 2, the *FGBG prompt* achieves 5.6 CHAIR, 27.8 HAL, and 2.6 Cog scores using InstructBLIP on the AMBER dataset. Similarly, mPLUG-Owl2 shows low hallucination results with 5.6 CHAIR, 26.5 HAL, and 2.1 Cog scores. The improved results with low hallucination did not compromise coverage, with the highest 53.2 and 54.3 Cover scores using InstructBLIP and mPLUG-Owl2, respectively, indicating a more precise response correction ability compared to other baseline methods. Additionally, the *FGBG prompt* outperforms the baselines with significantly lower CH_s and CH_i scores for both LVLMs. InstructBLIP shows a 31.2% reduction in CH_s and 9.1% reduction in CH_i , while mPLUG-Owl2 demonstrates a 30.0% reduction in CH_s and 8.0% reduction in CH_i , indicating an overall relative hallucination reduction of around 50%.

We examine the two-step results of *FGBG prompt*. LVLMs generally respond to the *FG prompt* with short responses similar to image captioning. This leads to notably low CHAIR, HAL, and Cog scores on the AMBER dataset using InstructBLIP (2.2, 4.5, and 0.2) and mPLUG-Owl2 (3.9, 14.1, and 0.7). In contrast, the *BG prompt* induces more hallucinations compared to the FG, with CHAIR scores increasing by 6.4% and 7.8%. The higher HAL scores (27.1% with InstructBLIP and 19.6% with mPLUG-Owl2) further indicate uncertainty in background descrip-

tions. However, *FG prompt* results in a Cover score reduction of 16.5% and 10% with InstructBLIP and mPLUG-Owl2, respectively. A similar disadvantage is seen with the *Stopping prompt*, which leads to a Cover score decline of 5.7% and 3.3% using InstructBLIP and mPLUG-Owl2, respectively. These results are intriguing, as the LVLMs continue to hallucinate even when informed that certain objects do not exist. This suggests a tradeoff between being verbose and conservative for LVLMs. Notably, InstructBLIP tends to replicate foreground descriptions more frequently, resulting in higher Cover scores. However, when combined with foreground descriptions, the results are not superior to those of mPLUG-Owl2. Another noteworthy observation is that the effects of hallucination reduction are not uniform across each Z_o .

Figure 5 illustrates a case where image-pasting eliminates the hallucination, while FGBG continues to hallucinate, suggesting a complex cross-modality causal interaction. To specifically examine the intervention’s effect on the hallucinatory-inducing word, we also measure the change in CHAIR scores for an object Z_o conditioned on the hallucinatory-inducing word. The results are reported in the Supplementary.

4.3. Evaluation of Embedding Intervention

The quantitative evaluation of our embedding intervention approach (§3.6) is reported in Table 2. Compared to the baseline results on the AMBER dataset, *Embedding* reduces a 5.2% HAL score while maintaining a 52.7% Cover score for InstructBLIP. Meanwhile, *Embedding* results for mPLUG-Owl2 sacrifices 1.1% Cover score but achieves a 7% reduction in the HAL score. Promising results are observed on the COCO dataset which achieves declined CHAIR scores with kept recall scores.

Saliency visualization: Figure 4 visualizes the calculated embedding saliency map M described in §3.6. The salient dimensions can be observed in light green for pos-

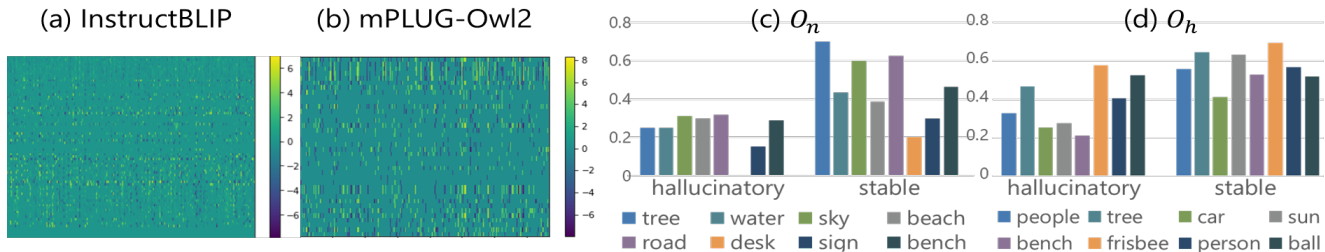


Figure 4. Embedding Saliency with timestamps in rows and dimensions in columns for (a) Instructblip and (b) mPLUG-Owl2. (c) and (d) show retrieval safe scores given either a non-hallucinatory word (O_n) or a commonly hallucinatory word (O_h) described in §4.3 using InstructBLIP on AMBER dataset.



InstructBLIP "In the image, a young boy is running through a lush green field, holding a **frisbee** in his hand. He appears to be enjoying himself as he runs and throws the **frisbee** back and forth. There are several other people in the scene, but they are not actively participating in the **frisbee** game. The grassy field is filled with various patches of green, creating a vibrant and lively setting for the young boy's playtime."

Image pasting (+) "In the image, a young boy is running across a grassy field with a white rabbit in the background. The boy is wearing a striped shirt and appears to be enjoying his time in the outdoors. The rabbit is positioned towards the right side of the image, adding a playful touch to the scene."

FGBG (-) "a toddler playing with a **frisbee** in a grassy field. In the image, a young boy is running across a grassy field, holding a **frisbee** in his hand. He appears to be enjoying himself as he runs and throws the **frisbee** around. There are several other people in the background, but they are not actively participating in the **frisbee** game."

Figure 5. A case with the FGBG approach continuing to hallucinate while image-pasting successfully reduces the hallucination, indicating the potential to explore cross-modality causal relations.

itive values ($e_h > e_n$) and dark blue for negative values ($e_h < e_n$) given the index (i, j) with embedding values $e_h = E_h(i, j)$ and $e_n = e_n(i, j)$. The sparsity of the saliency map illuminates the limited underlying causal feature dimensions affecting hallucination. The visualized results averaging over attention heads are shown in Figure 4 and the other figures for different heads, timestamps, and dimensions are reported in the supplementary.

Embedding property analysis: In the previous experiments, a few data are less likely to be hallucinated which can be used as stable targets to assess the property of an embedding. Specifically, we regard a group of data X_{stable} that is never hallucinated with our three text prompts in §4.2. When an arbitrary embedding E retrieves its nearest neighbors E_0 , we can identify if E_0 is in the X_{stable} . For a sample set, we obtain a ratio of the retrieved data belonging to X_{stable} and term this ratio as a "retrieval safe score". A higher retrieval safe score signifies that this set of embeddings is located near less hallucinated samples.

We regard the cases that comprise either a common hallucinatory-inducing word (O_n) or a hallucinatory word (O_h) described in §3.2 narrated in the response. The word can occur in a response that belongs to a group X_h being hallucinated with the raw LVLm inference or the stable group X_{stable} less likely to be hallucinated. Figure 4 (c) demonstrates the results of O_n within the groups of X_h or X_{stable} and (d) shows O_h results.

In both Figure 4 (c) and (d), X_h consistently yields lower retrieval safety scores than X_{stable} , indicating distinct properties in the embedding space. Aside from the general finding, it is necessary to consider the scores under the condi-

tion that a given word occurred in that the contexts might be specified differently. Figure 4 (c) shows that samples mentioned 'desk' and 'sign' attain low scores in X_{stable} yet still higher than the scores in X_h . A given word of O_n in Figure 4 (c) exhibits consistently low safe scores for X_{stable} while O_h in Figure 4 (d) includes unexpected high safe scores such as the frisbee. That is, O_n stands closer to hallucinatory embeddings while O_h does not. This suggests that non-hallucinatory objects (O_n) pose hidden risks for inducing hallucinations, offering new insights into managing hallucinations via embedding space.

5. Conclusion

We introduce a causal hallucination probing scheme to analyze potential approaches to mitigate hallucination and identify the underlying hallucination structure that non-hallucinatory objects can induce hallucination. Our analyses explore image, text, and embedding interventions in the causal framework that can block unwanted causality relations of the inducing objects. Our proposed simple approaches achieve significant reduction over other hallucination mitigation methods without model parameter updating. Further, our investigation in embedding intervention uncovers the potential to manipulate the representation space directly. For future works, we will apply causal effects to more complex multimodal tasks and unveil the complex relation in large-scale training and testing datasets. Further exploring the cross-modality causality and model internals in reflecting hallucination under various circumstances is still critical research to extend this study.

References

- [1] Josh Achiam, Steven Adler, Sandhini Agarwal, Lama Ahmad, Ilge Akkaya, Florencia Leoni Aleman, Diogo Almeida, Janko Altenschmidt, Sam Altman, Shyamal Anadkat, et al. GPT-4 technical report. *arXiv preprint arXiv:2303.08774*, 2023. **3**
- [2] Zechen Bai, Pichao Wang, Tianjun Xiao, Tong He, Zongbo Han, Zheng Zhang, and Mike Zheng Shou. Hallucination of multimodal large language models: A survey. *arXiv preprint arXiv:2404.18930*, 2024. **1**
- [3] Satyanjeev Banerjee and Alon Lavie. Meteor: An automatic metric for mt evaluation with improved correlation with human judgments. In *Proceedings of the acl workshop on intrinsic and extrinsic evaluation measures for machine translation and/or summarization*, pages 65–72, 2005. **2**
- [4] Ali Furkan Biten, Lluís Gómez, and Dimosthenis Karatzas. Let there be a clock on the beach: Reducing object hallucination in image captioning. In *Proceedings of the IEEE/CVF Winter Conference on Applications of Computer Vision*, pages 1381–1390, 2022. **1**
- [5] Jiali Chen, Zhenjun Guo, Jiayuan Xie, Yi Cai, and Qing Li. Deconfounded visual question generation with causal inference. In *Proceedings of the 31st ACM International Conference on Multimedia*, pages 5132–5142, 2023. **3**
- [6] Zhongzhi Chen, Xingwu Sun, Xianfeng Jiao, Fengzong Lian, Zhanhui Kang, Di Wang, and Chengzhong Xu. Truth forest: Toward multi-scale truthfulness in large language models through intervention without tuning. In *Proceedings of the AAAI Conference on Artificial Intelligence*, volume 38, pages 20967–20974, 2024. **3**
- [7] Siyuan Cheng, Bozhong Tian, Qingbin Liu, Xi Chen, Yongheng Wang, Huajun Chen, and Ningyu Zhang. Can we edit multimodal large language models? In *Proceedings of the 2023 Conference on Empirical Methods in Natural Language Processing*, pages 13877–13888, Singapore, Dec. 2023. Association for Computational Linguistics. **6**
- [8] Wenliang Dai, Junnan Li, Dongxu Li, Anthony Meng Huat Tiong, Junqi Zhao, Weisheng Wang, Boyang Li, Pascale N Fung, and Steven Hoi. Instructblip: Towards general-purpose vision-language models with instruction tuning. *Advances in Neural Information Processing Systems*, 36, 2024. **1, 2, 3, 6**
- [9] Anisha Gunjal, Jihan Yin, and Erhan Bas. Detecting and preventing hallucinations in large vision language models. In *Proceedings of the AAAI Conference on Artificial Intelligence*, volume 38, pages 18135–18143, 2024. **2**
- [10] Qidong Huang, Xiaoyi Dong, Pan Zhang, Bin Wang, Conghui He, Jiaqi Wang, Dahua Lin, Weiming Zhang, and Nenghai Yu. Opera: Alleviating hallucination in multimodal large language models via over-trust penalty and retrospection-allocation. *arXiv preprint arXiv:2311.17911*, 2023. **3, 6**
- [11] Chaoya Jiang, Haiyang Xu, Mengfan Dong, Jiaying Chen, Wei Ye, Ming Yan, Qinghao Ye, Ji Zhang, Fei Huang, and Shikun Zhang. Hallucination augmented contrastive learning for multimodal large language model. *arXiv preprint arXiv:2312.06968*, 2023. **1**
- [12] Jae Myung Kim, A. Sophia Koepke, Cordelia Schmid, and Zeynep Akata. Exposing and mitigating spurious correlations for cross-modal retrieval. In *Proceedings of the IEEE/CVF Conference on Computer Vision and Pattern Recognition (CVPR) Workshops*, pages 2585–2595, June 2023. **1**
- [13] Seongyun Lee, Sue Hyun Park, Yongrae Jo, and Minjoon Seo. Volcano: mitigating multimodal hallucination through self-feedback guided revision. *arXiv preprint arXiv:2311.07362*, 2023. **2**
- [14] Sicong Leng, Hang Zhang, Guanzheng Chen, Xin Li, Shijian Lu, Chunyan Miao, and Lidong Bing. Mitigating object hallucinations in large vision-language models through visual contrastive decoding. *arXiv preprint arXiv:2311.16922*, 2023. **1, 3, 6**
- [15] Kenneth Li, Oam Patel, Fernanda Viégas, Hanspeter Pfister, and Martin Wattenberg. Inference-time intervention: Eliciting truthful answers from a language model. In *Thirty-seventh Conference on Neural Information Processing Systems*, 2023. **3, 6**
- [16] Yifan Li, Yifan Du, Kun Zhou, Jinpeng Wang, Wayne Xin Zhao, and Ji-Rong Wen. Evaluating object hallucination in large vision-language models. In *Proceedings of the 2023 Conference on Empirical Methods in Natural Language Processing*, pages 292–305, 2023. **2**
- [17] Tsung-Yi Lin, Michael Maire, Serge Belongie, James Hays, Pietro Perona, Deva Ramanan, Piotr Dollár, and C Lawrence Zitnick. Microsoft coco: Common objects in context. In *Computer Vision—ECCV 2014: 13th European Conference, Zurich, Switzerland, September 6–12, 2014, Proceedings, Part V 13*, pages 740–755. Springer, 2014. **3**
- [18] Zhiqiu Lin, Xinyue Chen, Deepak Pathak, Pengchuan Zhang, and Deva Ramanan. Revisiting the role of language priors in vision-language models. 2024. **3**
- [19] Bing Liu, Dong Wang, Xu Yang, Yong Zhou, Rui Yao, Zhiwen Shao, and Jiaqi Zhao. Show, deconfound and tell: Image captioning with causal inference. In *Proceedings of the IEEE/CVF Conference on Computer Vision and Pattern Recognition*, pages 18041–18050, 2022. **3**
- [20] Fuxiao Liu, Kevin Lin, Linjie Li, Jianfeng Wang, Yaser Yacoob, and Lijuan Wang. Mitigating hallucination in large multi-modal models via robust instruction tuning. In *The Twelfth International Conference on Learning Representations*, 2023. **2**
- [21] Haotian Liu, Chunyuan Li, Qingyang Wu, and Yong Jae Lee. Visual instruction tuning. In *NeurIPS*, 2023. **1, 2**
- [22] Hanchao Liu, Wenyan Xue, Yifei Chen, Dapeng Chen, Xiutian Zhao, Ke Wang, Liping Hou, Rongjun Li, and Wei Peng. A survey on hallucination in large vision-language models. *arXiv preprint arXiv:2402.00253*, 2024. **1**
- [23] Shilong Liu, Zhaoyang Zeng, Tianhe Ren, Feng Li, Hao Zhang, Jie Yang, Chunyuan Li, Jianwei Yang, Hang Su, Jun Zhu, et al. Grounding dino: Marrying dino with grounded pre-training for open-set object detection. *arXiv preprint arXiv:2303.05499*, 2023. **5**
- [24] Holy Lovenia, Wenliang Dai, Samuel Cahyawijaya, Ziwei Ji, and Pascale Fung. Negative object presence evaluation

- (nope) to measure object hallucination in vision-language models. *arXiv preprint arXiv:2310.05338*, 2023. 3
- [25] Vedant Palit, Rohan Pandey, Aryaman Arora, and Paul Pu Liang. Towards vision-language mechanistic interpretability: A causal tracing tool for blip. In *Proceedings of the IEEE/CVF International Conference on Computer Vision*, pages 2856–2861, 2023. 3
- [26] Judea Pearl. Direct and indirect effects. *Probabilistic and Causal Inference: The Works of Judea Pearl*, page 373, 2001. 4
- [27] Judea Pearl. *Causality*. Cambridge university press, 2009. 3, 4
- [28] Judea Pearl. The seven tools of causal inference, with reflections on machine learning. *Communications of the ACM*, 62:54 – 60, 2019. 4
- [29] Judea Pearl, Madelyn Glymour, and Nicholas P Jewell. *Causal inference in statistics: A primer*. John Wiley & Sons, 2016. 4, 5
- [30] Haoyi Qiu, Wenbo Hu, Zi-Yi Dou, and Nanyun Peng. Valoreval: Holistic coverage and faithfulness evaluation of large vision-language models. *arXiv preprint arXiv:2404.13874*, 2024. 2
- [31] Anna Rohrbach, Lisa Anne Hendricks, Kaylee Burns, Trevor Darrell, and Kate Saenko. Object hallucination in image captioning. In Ellen Riloff, David Chiang, Julia Hockenmaier, and Jun’ichi Tsujii, editors, *Proceedings of the 2018 Conference on Empirical Methods in Natural Language Processing*, pages 4035–4045, Brussels, Belgium, Oct.-Nov. 2018. Association for Computational Linguistics. 3
- [32] Alessandro Stolfo, Zhijing Jin, Kumar Shridhar, Bernhard Schoelkopf, and Mrinmaya Sachan. A causal framework to quantify the robustness of mathematical reasoning with language models. In *Proceedings of the 61st Annual Meeting of the Association for Computational Linguistics (Volume 1: Long Papers)*, pages 545–561, 2023. 4
- [33] Zhiqing Sun, Sheng Shen, Shengcao Cao, Haotian Liu, Chunyuan Li, Yikang Shen, Chuang Gan, Liang-Yan Gui, Yu-Xiong Wang, Yiming Yang, et al. Aligning large multi-modal models with factually augmented rlhf. *arXiv preprint arXiv:2309.14525*, 2023. 2
- [34] Ramakrishna Vedantam, C Lawrence Zitnick, and Devi Parikh. Cider: Consensus-based image description evaluation. In *Proceedings of the IEEE conference on computer vision and pattern recognition*, pages 4566–4575, 2015. 2
- [35] Ali Vosoughi, Shijian Deng, Songyang Zhang, Yapeng Tian, Chenliang Xu, and Jiebo Luo. Cross modality bias in visual question answering: A causal view with possible worlds vqa. *IEEE Transactions on Multimedia*, 2024. 3
- [36] Bin Wang, Fan Wu, Xiao Han, Jiahui Peng, Huaping Zhong, Pan Zhang, Xiaoyi Dong, Weijia Li, Wei Li, Jiaqi Wang, et al. Vigc: Visual instruction generation and correction. In *Proceedings of the AAAI Conference on Artificial Intelligence*, volume 38, pages 5309–5317, 2024. 2
- [37] Junyang Wang, Yuhang Wang, Guohai Xu, Jing Zhang, Yukai Gu, Haitao Jia, Ming Yan, Ji Zhang, and Jitao Sang. An LLM-free multi-dimensional benchmark for MLLMs hallucination evaluation. *arXiv preprint arXiv:2311.07397*, 2023. 3, 6
- [38] Junfei Wu, Qiang Liu, Ding Wang, Jinghao Zhang, Shu Wu, Liang Wang, and Tieniu Tan. Logical closed loop: Uncovers object hallucinations in large vision-language models. *arXiv preprint arXiv:2402.11622*, 2024. 1
- [39] Kelvin Xu, Jimmy Ba, Ryan Kiros, Kyunghyun Cho, Aaron Courville, Ruslan Salakhudinov, Rich Zemel, and Yoshua Bengio. Show, attend and tell: Neural image caption generation with visual attention. In *International conference on machine learning*, pages 2048–2057. PMLR, 2015. 5
- [40] Peng Xu, Wenqi Shao, Kaipeng Zhang, Peng Gao, Shuo Liu, Meng Lei, Fanqing Meng, Siyuan Huang, Yu Qiao, and Ping Luo. Lvlm-ehub: A comprehensive evaluation benchmark for large vision-language models. *arXiv preprint arXiv:2306.09265*, 2023. 2
- [41] Siming Yan, Min Bai, Weifeng Chen, Xiong Zhou, Qixing Huang, and Li Erran Li. Vigor: Improving visual grounding of large vision language models with fine-grained reward modeling. *arXiv preprint arXiv:2402.06118*, 2024. 2
- [42] Xu Yang, Hanwang Zhang, and Jianfei Cai. Deconstructed image captioning: A causal retrospect. *IEEE Transactions on Pattern Analysis and Machine Intelligence*, 45(11):12996–13010, 2021. 3
- [43] Xu Yang, Hanwang Zhang, Guojun Qi, and Jianfei Cai. Causal attention for vision-language tasks. In *Proceedings of the IEEE/CVF conference on computer vision and pattern recognition*, pages 9847–9857, 2021. 3
- [44] Qinghao Ye, Haiyang Xu, Guohai Xu, Jiabo Ye, Ming Yan, Yiyang Zhou, Junyang Wang, Anwen Hu, Pengcheng Shi, Yaya Shi, et al. mPLUG-Owl: Modularization empowers large language models with multimodality. *arXiv preprint arXiv:2304.14178*, 2023. 2
- [45] Qinghao Ye, Haiyang Xu, Jiabo Ye, Ming Yan, Haowei Liu, Qi Qian, Ji Zhang, Fei Huang, and Jingren Zhou. mPLUG-Owl2: Revolutionizing multi-modal large language model with modality collaboration. *arXiv preprint arXiv:2311.04257*, 2023. 1, 2, 3, 6
- [46] Shukang Yin, Chaoyou Fu, Sirui Zhao, Tong Xu, Hao Wang, Dianbo Sui, Yunhang Shen, Ke Li, Xing Sun, and Enhong Chen. Woodpecker: Hallucination correction for multimodal large language models. *arXiv preprint arXiv:2310.16045*, 2023. 2
- [47] Qifan Yu, Juncheng Li, Longhui Wei, Liang Pang, Wentao Ye, Bosheng Qin, Siliang Tang, Qi Tian, and Yueting Zhuang. Hallucidoctor: Mitigating hallucinatory toxicity in visual instruction data. *arXiv preprint arXiv:2311.13614*, 2023. 1, 2
- [48] Tao Yu, Runsen Feng, Ruoyu Feng, Jinming Liu, Xin Jin, Wenjun Zeng, and Zhibo Chen. Inpaint anything: Segment anything meets image inpainting. *ArXiv*, abs/2304.06790, 2023. 5
- [49] Tianyu Yu, Yuan Yao, Haoye Zhang, Taiwen He, Yifeng Han, Ganqu Cui, Jinyi Hu, Zhiyuan Liu, Hai-Tao Zheng, Maosong Sun, et al. Rlhf-v: Towards trustworthy mlms via behavior alignment from fine-grained correctional human feedback. *arXiv preprint arXiv:2312.00849*, 2023. 1
- [50] Congzhi Zhang, Linhai Zhang, Deyu Zhou, and Guoqiang Xu. Causal prompting: Debiasing large language model

- prompting based on front-door adjustment. *arXiv preprint arXiv:2403.02738*, 2024. 5
- [51] Linxi Zhao, Yihe Deng, Weitong Zhang, and Quanquan Gu. Mitigating object hallucination in large vision-language models via classifier-free guidance. *arXiv preprint arXiv:2402.08680*, 2024. 2
- [52] Fan Zhou, Yuzhou Mao, Liu Yu, Yi Yang, and Ting Zhong. Causal-debias: Unifying debiasing in pretrained language models and fine-tuning via causal invariant learning. In *Proceedings of the 61st Annual Meeting of the Association for Computational Linguistics (Volume 1: Long Papers)*, pages 4227–4241, 2023. 3
- [53] Yiyang Zhou, Chenhang Cui, Jaehong Yoon, Linjun Zhang, Zhun Deng, Chelsea Finn, Mohit Bansal, and Huaxiu Yao. Analyzing and mitigating object hallucination in large vision-language models. In *The Twelfth International Conference on Learning Representations*, 2024. 1, 5
- [54] Deyao Zhu, Jun Chen, Xiaoqian Shen, Xiang Li, and Mohamed Elhoseiny. MiniGPT-4: Enhancing vision-language understanding with advanced large language models. In *The Twelfth International Conference on Learning Representations*, 2023. 1, 2